AIMS Mathematics, 11(1): 1175–1201.
DOI: 10.3934/math.2026050
Received: 30 October 2025
Revised: 04 January 2026
Accepted: 09 January 2026
Published: 15 January 2026

https://www.aimspress.com/journal/Math

Research article

Analysis and anti-control of bifurcations in two-dimensional, three-parameter discrete dynamical system with cubic terms

Limei Liu, Jiangna Ruan*, Jun Zhai and Xiuling Li*

School of Statistics and Data Science, Jilin University of Finance and Economics, Changchun 130117, China

* **Correspondence:** Email: 5241091004@s.jlufe.edu.cn, lixiuling@jlufe.edu.cn.

Abstract: In this paper, we proposed a class of two-dimensional three-parameter discrete dynamical systems with cubic terms, which can be applied to image encryption. We present a study on the analysis and control of the bifurcations in these systems. Initially, the existence and stability conditions of the fixed points of the proposed systems were proposed. Subsequently, based on the center manifold and bifurcation theories, we determined the conditions for the existence of Neimark-Sacker, pitchfork, and period-doubling bifurcations. The bifurcation diagram and the phase portraits were employed in the numerical experiments to verify the correctness of theoretical analysis. Finally, anti-controllers were used to induce Neimark-Sacker and period-doubling bifurcations, which were designed by integrating the bifurcation conditions with the state feedback method. The proposed anti-controllers caused the systems to undergo the desired bifurcations at the preset parameter values. Numerical simulations verified the effectiveness and robustness of the proposed controllers.

Keywords: two-dimensional discrete dynamical system; stability; Neimark-Sacker bifurcation; period-doubling bifurcation; pitchfork bifurcation; anti-control
Mathematics Subject Classification: 39A28, 39A30, 39A33, 65P30, 93B52

1. Introduction

Discrete maps with cubic terms are widely utilized in various fields, including electronic circuits, chemical reactions, physical systems, and population genetics [1,2]. Their capacity to

generate rich bifurcation sequences and chaos makes them a persistent focus of nonlinear dynamics research. The evolution of this field reveals a progression from exploring intrinsic nonlinear effects in simple models to investigating their manifestation under specific structural constraints like coupling forms and invertibility. In this paper, we aim to advance this trajectory by proposing and analyzing a class of new two-dimensional discrete maps with cubic terms. To position our work, we discuss some dynamical effects central to the maps with cubic terms in the literature.

The foundational effect of a cubic term is a nonlinearity, which can induce complex bifurcations and chaos. Early studies established this in one-dimensional maps. In 1980, May introduced the cubic map

$$X_{t+1} = aX_t^3 + (1-a)X_t, \tag{1}$$

where a is a parameter, and the map is defined on the interval $I = [-1,1]$ [3]. Bifurcation sequences of period 2^n cycles exist in the system (1). As a result, their bifurcation structures are more complex than the logistic map. Further studies conducted in 1983 revealed that the cubic map exhibits snapback repellers and chaotic behaviors [4]. The researchers in [5] investigated a one-parameter, symmetric cubic map

$$X_{n+1} = X_n + \lambda X_n(1-X_n)(\tfrac{1}{2} - X_n), \tag{2}$$

where λ is a parameter ranging from 0 to 16. Periodic orbits and bifurcations are analyzed. As λ increases, the symmetric cubic map (2) undergoes the cycles bifurcations through subharmonic bifurcations. These works indicate that the pure effect of the cubic terms is a robust source of chaos and period-doubling cascades.

Extending to two-dimensional maps, the coupling effect is critical, which interacts with the cubic terms to define global dynamics. Research has evolved to explore various architectures. The researchers in [6,7] focused on studying the two-dimensional cubic Hénon map

$$\begin{cases} x_{n+1} = -y_n + x_n^3 + \mu x_n + 0.7, \\ y_{n+1} = x_n, \end{cases} \tag{3}$$

where μ is a parameter. This map undergoes a triplication at $\mu = -1.1505$ and has the saddle center collision at $\mu = -1.12189$. The researchers in [8] investigated the two-dimensional noninvertible map with cubic terms

$$\begin{cases} x \mapsto ax + y, \\ y \mapsto bx + x^3, \end{cases} \tag{4}$$

where $b < 0$. An analysis of the bifurcation and chaotic behaviors is presented. Two two-dimensional maps with cubic terms are derived from a one-dimensional cubic map

$$T_o(x) = x^3 + (a+1)x + b. \tag{5}$$

One is the two-dimensional map

$$T_1: \begin{cases} x_{n+1} = x_n^3 + (a+1)x_n + b + y_n, \\ y_{n+1} = cx_n, \end{cases} \tag{6}$$

where a, b, c are real parameters [9]. The other is the two-dimensional noninvertible map

$$T_2:\begin{cases}x_{n+1}=\varepsilon x_n^3+(a+1)x_n+b+hy_n,\\ y_{n+1}=cx_n+dy_n,\end{cases} \tag{7}$$

where $\varepsilon=1$ or $\varepsilon=-1, a,b,c,d,h,$ are real parameters. In map T_1, a variation of parameter c induces a period-doubling bifurcation, which leads to chaotic behavior. When the basin boundary intersects with the chaotic attractor, the interaction disrupts or reorganizes the basin of attraction. The critical curve of the map T_2 (of type $Z_1-Z_3-Z_1$) partitions the phase plane into three distinct regions. The concept of basin bifurcation encompasses various transitions, including the distinctions between connected and disconnected basins, as well as simply connected and multiply connected structures. This phenomenon also demonstrates the coexistence of multiple attractors. The researchers in [10] investigated a two-dimensional cubic map

$$\begin{cases}x_{n+1}=y_n,\\ y_{n+1}=\mu y_n-y_n^3-Jx_n,\end{cases} \tag{8}$$

where μ is a parameter. Wada bifurcation and the characteristics of partial Wada basin boundaries are investigated. Two distinct types of Wada bifurcation are identified. Moreover, the underlying mechanisms responsible for the formation of partial Wada basin boundaries are elucidated. Based on the two-dimensional cubic map (8), the two-dimensional symplectic maps

$$C_{\pm}^{J}:\begin{cases}\bar{x}=y,\\ \bar{y}=M_1+M_2y-Jx\pm y^3,\end{cases} \tag{9}$$

are studied, which show that the maps (9) have the bifurcations of cubic homoclinic tangencies [11]. Especially, when $J=1$, the conservative cubic Hénon maps

$$H_3^{\pm}:\begin{cases}\bar{x}=y,\\ \bar{y}=-x+M_1+M_2y\pm y^3,\end{cases} \tag{10}$$

were extensively studied in [12,13]. Moreover, 1:4 resonance unfolding has the so-called Arnold degeneracy for C_-. The map C_+ has a different type of degeneracy. Non-symmetric points are created and destroyed at pitchfork bifurcations [12]. Bifurcations under reversible perturbations give rise to four 3-periodic orbits, where two of them are symmetric and conservative, and the other two orbits are nonsymmetrical and compose symmetric couples of dissipative orbits. These local symmetry-breaking bifurcations can lead to mixed dynamics [13]. These works demonstrate that the effect of the map's coupling structure is as consequential as the nonlinearity.

The historical development outlined above shows that while the effects of cubic nonlinearity, bifurcation, and structure have been deeply studied, they have primarily been explored in maps where nonlinearity is typically confined to a single dimension. That is, cubic terms such as x^3 exclusively influence the iteration of their own variable, leading to weak coupling and limited nonlinear interaction between system variables. This leads to a predominantly self-focused nonlinear interaction, highlighting a lack of research on maps with strong, targeted cross-coupling between variables. To address this, we propose a class of cross-coupled, two-dimensional three-parameter discrete maps with cubic terms. In the proposed maps, the cubic term x^3 is intentionally designed to drive the update of the y variable, while the evolution of the x variable retains a linear feedback coupling. Owing to the advantages in structure preservation, numerical reliability, computational efficiency, and physical authenticity, invertible maps have broad application across fields, including engineering control systems [14,15], ecological and biological modeling [16,17], economic and

financial analysis [18], neuroscience [19], numerical analysis [20,21], and cryptography and secure communication [22]. Consequently, the maps proposed in this paper are constructed to be invertible.

The control and anti-control of bifurcations represent a pivotal research direction in nonlinear dynamics. Bifurcation control is concerned with suppressing or eliminating undesired bifurcations to maintain system stability [23,24]. Conversely, anti-control of bifurcations aims to deliberately induce specific bifurcations (such as Neimark-Sacker bifurcation or period-doubling bifurcation) at predetermined parameter values [25,26]. This intentional induction of complex dynamics, particularly chaos, is crucial for meeting practical needs in engineering. To leverage this, and to further enhance the chaotic complexity of the proposed maps with cubic terms, we design the anti-control strategy to deliberately trigger either a Neimark-Sacker or a period-doubling bifurcation, thereby enabling the reliable generation of chaos.

This paper is organized as follows: In Section 2, a two-dimensional, three-parameter discrete dynamical system with cubic term is introduced, and the existence and stability of its fixed points are analyzed. In Section 3, we investigate the bifurcations of the proposed system through theoretical analysis and numerical experiments. The existence of Neimark-Sacker, pitchfork, and period-doubling bifurcations is established, and the critical parameter conditions are derived. The numerical results confirm the validity of the theoretical analysis and further indicate the potential application of the system in image encryption. In Section 4, the state feedback controllers are designed to achieve anti-control of the Neimark-Sacker and period-doubling bifurcations, thereby effectively inducing desired complex dynamics. Numerical simulations verify the effectiveness and robustness of the proposed controllers. Finally, in Section 5, we summarize the major conclusions of this work.

2. Existence and stability of fixed points in the two-dimensional three-parameter discrete dynamical system with cubic terms

We consider a class of two-dimensional three-parameter discrete dynamical systems with cubic terms, all of which are invertible and defined as

$$\begin{cases} x_{n+1} = ax_n - y_n, \\ y_{n+1} = bx_n + cx_n^3, \end{cases} \tag{11}$$

where a, b, c are the parameters, $a \in \mathbb{R}$, $b \cdot c > 0$. In these systems, the sole source of nonlinearity is the cubic term x^3, which appears exclusively in the second equation and affects only the evolution of y. The first equation remains completely linear. This structure creates a cross-coupling between x and y. Parameter a controls the self-feedback of x and the coupling influence of y, parameter b regulates the linear driving strength of x on y, and parameter c is the only nonlinear strength parameter, influencing the system only through x^3. Consequently, the structure of these systems renders bifurcation analysis more straightforward.

The discrete system (11) can be rewritten as

$$F: \begin{cases} x \mapsto ax - y, \\ y \mapsto bx + cx^3. \end{cases} \tag{12}$$

Suppose (x_0, y_0) is a fixed point of two-dimensional three-parameter discrete dynamical system with cubic terms, then (x_0, y_0) satisfies the following equation:

$$\begin{cases} x_0 = ax_0 - y_0, \\ y_0 = bx_0 + cx_0^3. \end{cases} \tag{13}$$

The Jacobian matrix of the discrete dynamical system (12) at the fixed point (x_0, y_0) is

$$Df(x_0, y_0) = \begin{bmatrix} a & -1 \\ b + 3cx_0^2 & 0 \end{bmatrix}. \tag{14}$$

The characteristic equation of the Jacobian matrix (14) is $\lambda^2 - a\lambda + 3cx_0^2 + b = 0$. By solving Eq (13), the fixed points of the system (12) can be obtained as follows:

- if $\frac{a-b-1}{c} \leq 0$, two-dimensional three-parameter discrete dynamical system with cubic terms has the unique fixed point (0,0);
- if $\frac{a-b-1}{c} > 0$, two-dimensional three-parameter discrete dynamical system with cubic terms has three fixed points (0,0), $\left(\sqrt{\frac{a-b-1}{c}}, (a-1)\sqrt{\frac{a-b-1}{c}}\right)$, $\left(-\sqrt{\frac{a-b-1}{c}}, -(a-1)\sqrt{\frac{a-b-1}{c}}\right)$, where $|a-1| > |b|$, and $(a-1) \cdot c > 0$.

Next, let us discuss the stability of the fixed points in system (12).

We focus on investigating the bifurcations at the fixed point (0,0) as parameters vary. Therefore, in this section, we mainly study the stability of the fixed point (0,0). The Jacobian matrix at the fixed point (0,0) is $DF(0,0) = \begin{bmatrix} a & -1 \\ b & 0 \end{bmatrix}$. Its characteristic equation is $\lambda^2 - a\lambda + b = 0$, and the eigenvalues are $\lambda_1 = \frac{a+\sqrt{a^2-4b}}{2}$, $\lambda_2 = \frac{a-\sqrt{a^2-4b}}{2}$.

Based on the stability criterion, the stability of the fixed point (0,0) in the discrete system (12) is shown as follows:

Proposition 2.1. *Considering two-dimensional three-parameter discrete dynamical system with cubic terms* (12), *the stability of the fixed point* (0,0) *is listed as follows*:

1) *when* $a^2 = 4b$:*if* $|a| < 2$, *the fixed point* (0,0) *is a stable node*; *if* $|a| > 2$, *the fixed point* (0,0) *is an unstable node;*
2) *when* $a^2 < 4b$:*if* $b < 1$, *the fixed point* (0,0) *is a stable focus*; *if* $b > 1$, *the fixed point* (0,0) *is unstable focus*; *if* $b = 1$, *the fixed point* (0,0) *is a center;*
3) *when* $a^2 > 4b$:*if* $|1 + b| < |a|$, *the fixed point* (0,0) *is a saddle*; *if* $-1 < b < 1$, $b > a - 1$, $b > -a - 1$, *the fixed point* (0,0) *is a stable node*; *if* $a > 2, 1 < b < a - 1 or a < -2, 1 < b < -a - 1$ *or* $b < -1, 1 + b < a < -1 + b$, *the fixed point* (0,0) *is an unstable node.*

Summarizing the content of Proposition 2.1, we have summarized the following results:

Proposition 2.2. *If* $b > a - 1, b > -a - 1, -1 < b < 1$, *the fixed point* (0,0) *of two-dimensional discrete dynamical system* (12) is stable; otherwise, it is unstable.

3. Bifurcation analysis of two-dimensional, three-parameter discrete dynamical system with cubic terms

3.1. Existence analysis of bifurcations

3.1.1. Theoretical analysis of the existence of bifurcations

From the stability analysis of the fixed point (0,0) for system (12), it is found that $b = 1$, $b = a - 1$, $b = -a - 1$ are the key points for the change in stability of system (12). Therefore, the bifurcations of system (12) will be studied subsequently under the conditions of $b = 1, b = a - 1$, $b = -a - 1$.

Lemma 3.1. (*Neimark-Sacker bifurcation existence theorem for discrete dynamical system* [27].) *Let* $f_\mu: \mathbb{R}^2 \mapsto \mathbb{R}^2$ *be a one-parameter family of mappings which has a smooth family of fixed points* $x(\mu)$ *at which the eigenvalues are complex conjugates* $\lambda(\mu)$, $\bar{\lambda}(\mu)$. *Assume*

(SH1) $|\lambda(\mu_0)| = 1$, *but* $\lambda^j(\mu_0) \neq 1$ *for* $j = 1,2,3,4$.

(SH2) $\frac{d}{d\mu}(|\lambda(\mu_0)|) = d \neq 0$.

Then there is a smooth change of coordinates h *so that the expression of* $h \circ f_\mu \circ h^{-1}$ *in polar coordinates has the form*

$$h \circ f_\mu \circ h^{-1}(r, \theta) = (r(1 + d(\mu - \mu_0) + ar^2), \theta + c + br^2) \ + \textit{higher-order terms}.$$

(*Note:* λ *complex and* (SH2) *imply* $|arg(\lambda)| = c$ *and* d *are nonzero.*)

(SH3) $\alpha \neq 0$.

Then there is a two-dimensional surface Σ *(not necessarily infinitely differentiable) in* $\mathbb{R}^2 \times \mathbb{R}$ *having quadratic tangency with the plane* $\mathbb{R}^2 \times \{\mu_0\}$ *which is invariant for* f_μ. *If* $\Sigma \cap (\mathbb{R}^2 \times \{\mu\})$ *is larger than a point, then it is a simple closed curve.*

Assuming the bifurcating system (restricted to the center manifold) is in the form

$$\begin{pmatrix} x \\ y \end{pmatrix} \mapsto \begin{bmatrix} cos(c) & -sin(c) \\ sin(c) & cos(c) \end{bmatrix} \begin{pmatrix} x \\ y \end{pmatrix} + \begin{pmatrix} f(x,y) \\ g(x,y) \end{pmatrix}.$$

With eigenvalues $\lambda, \bar{\lambda} = e^{\pm ic}$, *one obtains*

$$\alpha = -Re\left[\frac{(1-2\lambda)\bar{\lambda}^2}{1-\lambda}\xi_{11}\xi_{20}\right] - \frac{1}{2}|\xi_{11}|^2 - |\xi_{02}|^2 + Re(\bar{\lambda}\xi_{21}),$$

where

$$\xi_{20} = \frac{1}{8}\left[(f_{xx} - f_{yy} + 2g_{xy}) + i(g_{xx} - g_{yy} - 2f_{xy})\right],$$

$$\xi_{11} = \frac{1}{4}\left[(f_{xx} + f_{yy}) + i(g_{xx} + g_{yy})\right],$$

$$\xi_{02} = \frac{1}{8}\left[(f_{xx} - f_{yy} - 2g_{xy}) + i(g_{xx} - g_{yy} + 2f_{xy})\right],$$

$$\xi_{21} = \frac{1}{16}\left[(f_{xxx} + f_{xyy} + g_{xxy} + g_{yyy}) + i(g_{xxx} + g_{xyy} - f_{xxy} - f_{yyy})\right].$$

Theorem 3.1. *If* $c > 0, -2 < a < 2$ *and* $a \neq -1,\ a \neq 0$, *the two-dimensional three-parameter discrete dynamical system with cubic terms* (12) *undergoes a Neimark-Sacker bifurcation at the fixed point* (0,0) *for* $b = 1$. *Moreover, there exists a unique repelling invariant closed curve, which bifurcates from the fixed point* (0,0).

Proof of Theorem 3.1. The Jacobian matrix at the fixed point (0,0) of system (12) is

$$DF(0,0) = \begin{bmatrix} a & -1 \\ b & 0 \end{bmatrix}.$$

For the eigenvalues $\lambda = \frac{a+\sqrt{a^2-4b}}{2}$ and $\bar{\lambda} = \frac{a-\sqrt{a^2-4b}}{2}$ to be a pair of complex conjugates and $|\lambda(b)| = 1$, it requires $b = 1$ and $-2 < a < 2$.

Through calculation, it is derived that if $a \neq -1,\ a \neq 0,\ [\lambda(1)]^n \neq 1$, where $n = 1,2,3,4$; and $\frac{d}{d(b)}(|\lambda(1)|) = \frac{1}{2} \neq 0$. When $-2 < a < 2$, let the invertible matrix

$$T = \begin{bmatrix} \frac{\sqrt{4-a^2}}{2} & \frac{a}{2} \\ 0 & 1 \end{bmatrix},\ T^{-1} = \begin{bmatrix} \frac{2}{\sqrt{4-a^2}} & -\frac{a}{\sqrt{4-a^2}} \\ 0 & 1 \end{bmatrix}.$$

We use the translation $\begin{pmatrix} x \\ y \end{pmatrix} = T\begin{pmatrix} u \\ v \end{pmatrix}$, and system (12) is transformed into

$$\begin{pmatrix} u \\ v \end{pmatrix} \mapsto \begin{pmatrix} \frac{a}{2} & -\frac{\sqrt{4-a^2}}{2} \\ \frac{\sqrt{4-a^2}}{2} & \frac{a}{2} \end{pmatrix}\begin{pmatrix} u \\ v \end{pmatrix} + \begin{pmatrix} f(u,v) \\ g(u,v) \end{pmatrix}.$$

Moreover,

$$f(u,v) = -\frac{ac}{\sqrt{4-a^2}}\left(\frac{a}{2}v + \frac{\sqrt{4-a^2}}{2}u\right)^3, g(u,v) = c\left(\frac{a}{2}v + \frac{\sqrt{4-a^2}}{2}u\right)^3.$$

According to Lemma 3.1, we can obtain

$$\xi_{20} = \left[\frac{3ac(u\sqrt{4-a^2}+av)}{8\sqrt{4-a^2}} + i\frac{3c(u\sqrt{4-a^2}+av)}{8}\right]\Big|_{u=0,v=0} = 0;$$

$$\xi_{11} = \left[-\frac{3ac(u\sqrt{4-a^2}+av)}{4\sqrt{4-a^2}} + i\frac{3c(u\sqrt{4-a^2}+av)}{4}\right]\Big|_{u=0,v=0} = 0;$$

$$\xi_{02} = \left[\begin{array}{l}(-\frac{9a^2cv\sqrt{4-a^2}}{32} + \frac{3a^3cu}{8} - \frac{9acu}{8} + \frac{3a^4cv}{32\sqrt{4-a^2}}) \\ +i(-\frac{3a^3cv}{8} + \frac{3acv}{8} - \frac{3a^2cu\sqrt{4-a^2}}{8} + \frac{3cu\sqrt{4-a^2}}{8})\end{array}\right]\Big|_{u=0,v=0} = 0;$$

$$\xi_{21} = i\frac{3c}{4\sqrt{4-a^2}};$$

$$\alpha = -\mathrm{Re}\left[\frac{(1-2\lambda)\bar{\lambda}^2}{1-\lambda}\xi_{11}\xi_{20}\right] - \frac{1}{2}\left|\xi_{11}\right|^2 - \left|\xi_{02}\right|^2 + \mathrm{Re}(\bar{\lambda}\xi_{21}) = \frac{3c}{8}.$$

Thus, when $-2 < a < 2$ and $a \neq -1$, $a \neq 0$, the two-dimensional three-parameter discrete dynamical system with cubic terms (12) undergoes a Neimark-Sacker bifurcation at the fixed point (0,0) for $b = 1$. In system (12), $c < 0$ is equivalent to $b < 0$. Therefore, when $c < 0$, Neimark-Sacker bifurcation at $b = 1$ needs not be considered. However, $c > 0$ is equivalent to $b > 0$. When $c > 0$, then $\alpha > 0$. The Neimark-Sacker bifurcation is subcritical; a closed curve exists, surrounding the fixed point (0,0) for $b < 1$ and $|b-1|$ small. Based on a comprehensive analysis, if $c > 0$, $-2 < a < 2$ and $a \neq -1$, $a \neq 0$, discrete dynamical system (12) undergoes a Neimark-Sacker bifurcation at the fixed point (0,0) for $b = 1$. Moreover, there exists a unique repelling invariant closed curve, which bifurcates from the fixed point (0,0).

Theorem 3.2.

(1) *If* $c < 0, a < 1$, *two-dimensional three-parameter discrete dynamical system with cubic terms* (12) *undergoes a pitchfork bifurcation at the fixed point* (0,0) *for* $b = a - 1$. *Moreover, three fixed points lie on the right of* $b = a - 1$ *and one fixed point lies on the left of* $b = a - 1$.

(2) *If* $c > 0, a > 1$, *and* $a \neq 2$, *two-dimensional three-parameter discrete dynamical system with cubic terms* (12) *undergoes a pitchfork bifurcation at the fixed point* (0,0) *for* $b = a - 1$. *Moreover, three fixed points lie on the left of* $b = a - 1$ *and one fixed point lies on the right of* $b = a - 1$.

Proof of Theorem 3.2. When $b = a - 1$, let $\bar{b} = b - (a-1)$.Taking $\bar{b}$ as an independent variable, system (12) is transformed into

$$\begin{cases} x \mapsto ax - y, \\ y \mapsto (a-1)x + \bar{b}x + cx^3, \\ \bar{b} \mapsto \bar{b}. \end{cases} \tag{15}$$

Let the invertible matrix $T = \begin{pmatrix} 1 & 1 & 0 \\ a-1 & 1 & 0 \\ 0 & 0 & 1 \end{pmatrix}$, and introduce the transformation

$$\begin{pmatrix} x \\ y \\ \bar{b} \end{pmatrix} = T\begin{pmatrix} u \\ v \\ w \end{pmatrix} = \begin{pmatrix} u+v \\ (a-1)u+v \\ w \end{pmatrix},$$

system (15) can be transformed into

$$\begin{pmatrix} u \\ v \\ w \end{pmatrix} \mapsto \begin{pmatrix} 1 & 0 & 0 \\ 0 & a-1 & 0 \\ 0 & 0 & 1 \end{pmatrix}\begin{pmatrix} u \\ v \\ w \end{pmatrix} + \begin{pmatrix} f(u,v,w) \\ g(u,v,w) \\ 0 \end{pmatrix}, \tag{16}$$

where

$$f(u,v,w)=\frac{1}{a-2}\Big[w(u+v)+c(u+v)^3\Big],$$
$$g(u,v,w)=\frac{1}{2-a}\Big[w(u+v)+c(u+v)^3\Big].$$

According to the center manifold theorem, we seek a center manifold

$$W^c(0)=\left\{(u,v,w)\in R^3 \mid v=h(u,w);h(0,0)=Dh(0,0)=0\right\}.$$

For u,w sufficiently small. We assume that $h(u,w)$ has the form

$$v=h(u,w)=a_1u^2+a_2uw+a_3w^2+a_4u^3+o\Big(\big(|u|+|w|\big)^3\Big). \tag{17}$$

The center manifold must satisfy the following equation:

$$N\big(h(u,w)\big)=h\Big[u+f\big(u,h(u,w),w\big),w\Big]-(a-1)h(u,w)-g\big(u,h(u,w),w\big)=0. \tag{18}$$

Balancing powers of coefficients of Eq (18), it is derived that

$$a_1=0,a_2=\frac{1}{(2-a)^2},a_3=0,a_4=\frac{c}{(2-a)^2}.$$

Hence, the center manifold is given by

$$v=\frac{1}{(2-a)^2}uw+\frac{c}{(2-a)^2}u^3+o\Big(\big(|u|+|w|\big)^3\Big). \tag{19}$$

The discrete dynamical system (16) restricted to $W^c(0)$ is given by

$$u\mapsto \overline{f}(u,w)=u+\frac{1}{a-2}uw+\frac{c}{a-2}u^3+o\Big(\big(|u|+|w|\big)^3\Big). \tag{20}$$

By calculating

$$\overline{f}(0,0)=0,\ \frac{\partial\overline{f}(0,0)}{\partial u}=1,\ \frac{\partial\overline{f}(0,0)}{\partial w}=0,$$

$$\frac{\partial^2\overline{f}(0,0)}{\partial u\partial w}=\frac{1}{a-2},\ \frac{\partial^2\overline{f}(0,0)}{\partial u^2}=0,\ \frac{\partial^3\overline{f}(0,0)}{\partial u^3}=\frac{6c}{a-2},$$

$$-\frac{\dfrac{\partial^3\overline{f}(0,0)}{\partial u^3}}{\dfrac{\partial^2\overline{f}(0,0)}{\partial u\partial w}}=-6c.$$

Since $c \neq 0$, as long as $a \neq 2$, system (20) undergoes a pitchfork bifurcation at $(u, w) = (0,0)$. Moreover, if $c < 0$, one of the curves of fixed points of system (20) lies on the right of $w = 0$; if $c > 0$, one of the curves of fixed points of system (20) lies on the left of $w = 0$ [28]. That is equivalent to if $a \neq 2$, then discrete dynamical system (12) undergoes a pitchfork bifurcation at the fixed point (0,0) for $b = a - 1$. When $c < 0$, it requires $b = a - 1 < 0$. When $c > 0$, it also requires $b = a - 1 > 0$. Based on a comprehensive analysis, if $c < 0, a < 1$, the discrete dynamical system (12) undergoes a pitchfork bifurcation at the fixed point (0,0) for $b = a - 1$. Moreover, three fixed points lie on the right of $b = a - 1$, and one fixed point lies on the left of $b = a - 1$. If $c > 0, a > 1$, and $a \neq 2$, discrete dynamical system (12) undergoes a pitchfork bifurcation at the fixed point (0,0) for $b = a - 1$. Moreover, three fixed points lie on the left of $b = a - 1$ and one fixed point lies on the right of $b = a - 1$.

Theorem 3.3.

(1) *If* $c < 0,\ a > -1$, *two-dimensional three-parameter discrete dynamical system with cubic terms* (12) *undergoes a period-doubling bifurcation at the fixed point* (0,0) *for* $b = -a - 1$. *Moreover*, *the period two points are unstable and lie on the right of* $b = -a - 1$.

(2) *If* $c > 0, a < -1$, *and* $a \neq -2$, *two-dimensional three-parameter discrete dynamical system with cubic terms* (12) *undergoes a pitchfork bifurcation at the fixed point* (0,0) *for* $b = -a - 1$. *Moreover, the period two points are stable and lie on the left of* $b = -a - 1$.

Proof of Theorem 3.3. When $b = -a - 1$, let $\bar{b} = b + a + 1$. Taking $\bar{b}$ as an independent variable, $b = \bar{b} - a - 1$, system (12) is transformed into

$$\begin{cases} x \mapsto ax - y, \\ y \mapsto (-a-1)x + \bar{b}x + cx^3, \\ \bar{b} \mapsto \bar{b}. \end{cases} \tag{21}$$

Let the invertible matrix $T = \begin{pmatrix} 1 & 1 & 0 \\ 1+a & -1 & 0 \\ 0 & 0 & 1 \end{pmatrix}$, and introduce the transformation

$$\begin{pmatrix} x \\ y \\ \bar{b} \end{pmatrix} = T \begin{pmatrix} u \\ v \\ w \end{pmatrix} = \begin{pmatrix} u+v \\ (1+a)u - v \\ w \end{pmatrix}.$$

System (21) can be transformed into

$$\begin{pmatrix} u \\ v \\ w \end{pmatrix} \mapsto \begin{pmatrix} -1 & 0 & 0 \\ 0 & a+1 & 0 \\ 0 & 0 & 1 \end{pmatrix} \begin{pmatrix} u \\ v \\ w \end{pmatrix} + \begin{pmatrix} f(u,v,w) \\ g(u,v,w) \\ 0 \end{pmatrix}, \tag{22}$$

where

$$f(u,v,w)=\frac{1}{a+2}w(u+v)+\frac{c}{a+2}(u+v)^3,$$

$$g(u,v,w)=-\frac{1}{a+2}w(u+v)-\frac{c}{a+2}(u+v)^3.$$

According to the center manifold theorem, we seek a center manifold

$$W^c(0)=\{(u,v,w)\in R^3 \mid v=h(u,w), h(0,0)=0, Dh(0,0)=0\}.$$

For u,w sufficiently small. We assume that $h(u,w)$ has the form

$$v=h(u,w)=b_1u^2+b_2uw+b_3w^2+b_4u^3+o\left(\left(|u|+|w|\right)^3\right). \tag{23}$$

The center manifold must satisfy the following equation:

$$N(h(u,w))=h\left[-u+f(u,h(u,w),w),w\right]-(a+1)h(u,w)-g(u,h(u,w),w)=0. \tag{24}$$

Through calculation, it is derived that

$$b_1=0, b_2=\frac{1}{(a+2)^2}, b_3=0, b_4=\frac{c}{(a+2)^2}.$$

Thus, the center manifold is given by

$$v=\frac{1}{(a+2)^2}uw+\frac{c}{(a+2)^2}u^3+o\left(\left(|u|+|w|\right)^3\right). \tag{25}$$

System (22) restricted to $W^c(0)$ is given by

$$u\mapsto \bar{f}(u,w)=-u+\frac{1}{a+2}uw+\frac{c}{a+2}u^3+o\left(\left(|u|+|w|\right)^3\right). \tag{26}$$

The second iterate of $\bar{f}(u,w)$ is given by

$$u\mapsto \bar{f}^2(u,w)=u-\frac{2}{a+2}uw-\frac{2c}{a+2}u^3+o\left(\left(|u|+|w|\right)^3\right). \tag{27}$$

It is sufficient for (26) and (27) to satisfy

$$\bar{f}(0,0)=0,\ \frac{\partial\bar{f}(0,0)}{\partial u}=-1,\ \frac{\partial\bar{f}^2(0,0)}{\partial w}=0,$$

$$\frac{\partial^2\bar{f}^2(0,0)}{\partial u^2}=0,\ \frac{\partial^2\bar{f}^2(0,0)}{\partial u\partial w}=-\frac{2}{a+2},\ \frac{\partial^3\bar{f}^2(0,0)}{\partial u^3}=-\frac{12c}{a+2},$$

$$-\frac{\frac{\partial^3 \overline{f}(0,0)}{\partial u^3}}{\frac{\partial^2 \overline{f}(0,0)}{\partial u \partial w}} = -6c.$$

Since $c \neq 0$, according to the bifurcation theory, as long as $a \neq -2$, system (26) undergoes a period-doubling bifurcation at $(u, w) = (0,0)$. Moreover, if $c < 0$, the period points are unstable and lie on the right of $w = 0$; if $c > 0$, the period points are stable and lie on the left of $w = 0$. It is equivalent that if $a \neq -2$, system (12) undergoes a period-doubling bifurcation at the fixed point (0,0) for $b = -a - 1$. When $c < 0$, the period points lie on the right of $b = -a - 1$. When $c > 0$, the period points lie on the left of $b = -a - 1$. However, system (12) requires that $bc > 0$.Therefore, when $c < 0$, then $b = -a - 1 < 0$; when $c > 0$, then $b = -a - 1 > 0$. Based on a comprehensive analysis, if $c < 0, a > -1$, system (12) undergoes a period-doubling bifurcation at the fixed point (0,0) for $b = -a - 1$, and the period points are unstable and lie on the right of $b = -a - 1$. If c > 0, a < –1, and $a \neq -2$, system (12) undergoes a period-doubling bifurcation at the fixed point (0,0) for $b = -a - 1$, and the period points are stable and lie on the left of $b = -a - 1$.

3.1.2. Numerical experiment of the existence of bifurcations

In Section 3.1.1, we derive the critical parameter conditions for Neimark-Sacker, pitchfork, and period-doubling bifurcations in system (12) through theoretical analysis. To validate the theoretical analysis, a series of numerical experiments are conducted in this section.

To verify the existence conditions of the Neimark-Sacker bifurcation, a set of numerical experiments are conducted with a = –0.2, b = 1, and c = 0.4. The initial state is (0.01,0.01). The results of the experiments are shown in Figures 1 and 2. Figure 1 is the phase portrait of an invariant circle for $b = 1$. Figure 2 lists two Lyapunov exponents of discrete system (12) with varying c. From Figure 2, one of the Lyapunov exponents is positive with $c > 0$. This means that system (12) is unstable as $c > 0$. These results are consistent with Theorem 3.1. When $c > 0$, the increase of c may lead system (12) to have chaotic behavior.

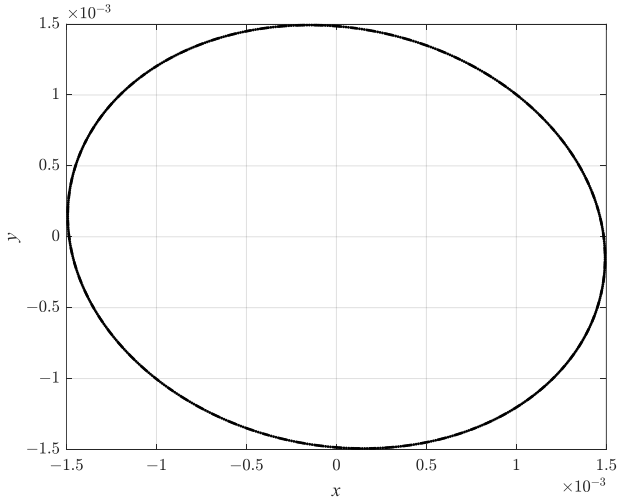

Figure 1. Phase portrait of discrete system (12) for a= –0.2, b = 1, and c = 0.4.

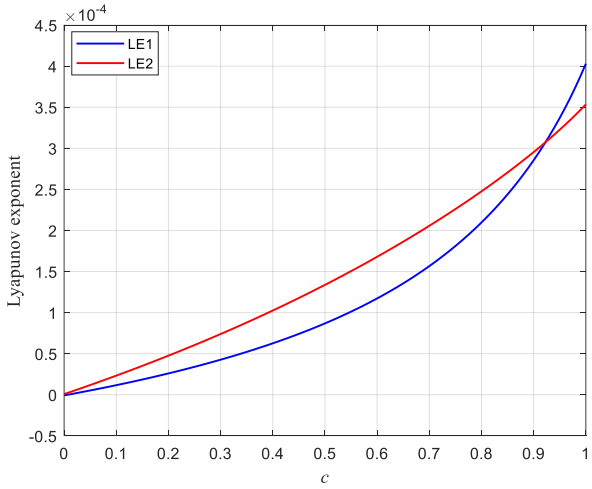

Figure 2. Lyapunov exponents of discrete system (12) at a = –0.2 and b = 1.

Two sets of experiments are conducted to verify the correctness of Theorem 3.2. The initial state is (0.01,0.01). Figure 3 illustrates the output x_0 of the first component of the fixed point (x_0, y_0) as varying b. The blue line shows the trivial fixed point branch, and the red curve shows the nontrivial fixed point branch. As such, when $a = -0.2, c = -0.4$, system (12) undergoes a pitchfork bifurcation at $b = -1.2$, and one of the curves of the fixed points of (12) lies on the right of $b = -1.2$. When $a = 2.5$, $c = 0.4$, system (12) undergoes a pitchfork bifurcation at $b = 1.5$, and one of the curves of fixed points of system (12) lies on the left of $b = 1.5$. These results are consistent with the results of Theorem 3.2. Figure 4 illustrates the maximum eigenvalue modulus of the Jacobian matrix $DF(0,0)$. From Figure 4, we obtain the stability of the trivial fixed point (0,0) with varying b. The results of stability are in accordance with Proposition 2.2.

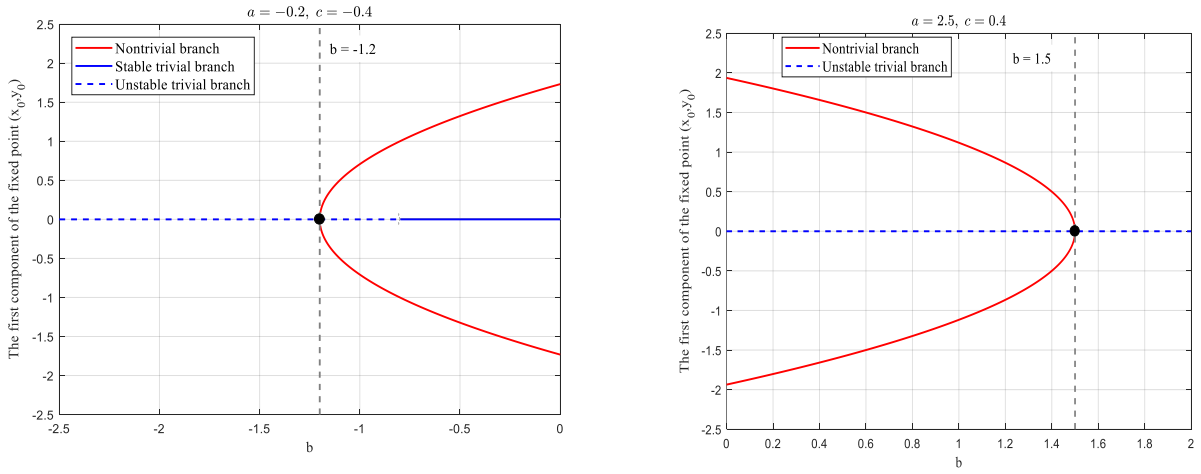

Figure 3. Output of the first component of the fixed point (x_0, y_0) with respect to b.

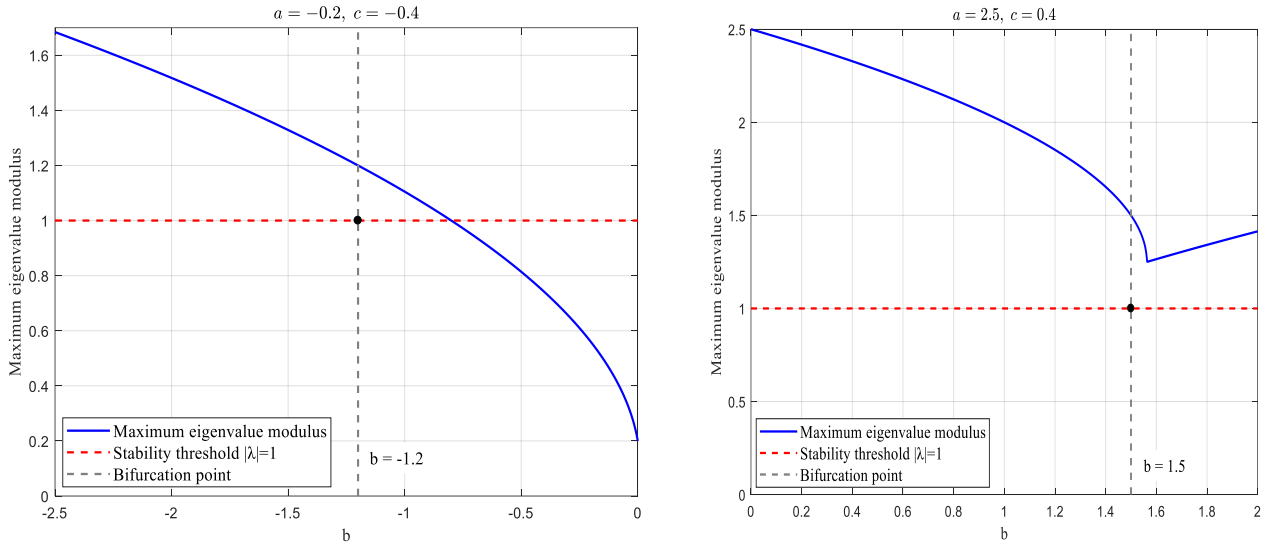

Figure 4. Maximum eigenvalue modulus of the Jacobian matrix at $(0,0)$ with respect to b.

To verify the correctness of Theorem 3.3, two sets of experiments are conducted with $a = -1.8,\ c = 0.5$ and $a = -0.5,\ c = -0.8$. The initial state is (0.01,0.01) in the experiments. The results of the numerical experiments are shown in Figures 5 and 6. Figure 5 shows the variations of the first component of the system state (x, y) with respect to b under different parameter values. This indicates that when a = –1.8 and c = 0.5, system (12) undergoes a period-doubling bifurcation at $b = 0.8$, and the period points lie on the left of $b = 0.8$. Moreover, when a = –0.5 and c = –0.8, system (12) undergoes a period-doubling bifurcation at $b = -0.5$, and the period points lie on the left of $b = -0.5$. These results are consistent with Theorem 3.3. When $b < -0.5$, Lyapunov exponents tend to infinity. Therefore, this is not shown in Figure 6. Figure 6 shows that $b = 0.8$ is a supercritical bifurcation point, and $b = -0.5$ is a subcritical bifurcation point.

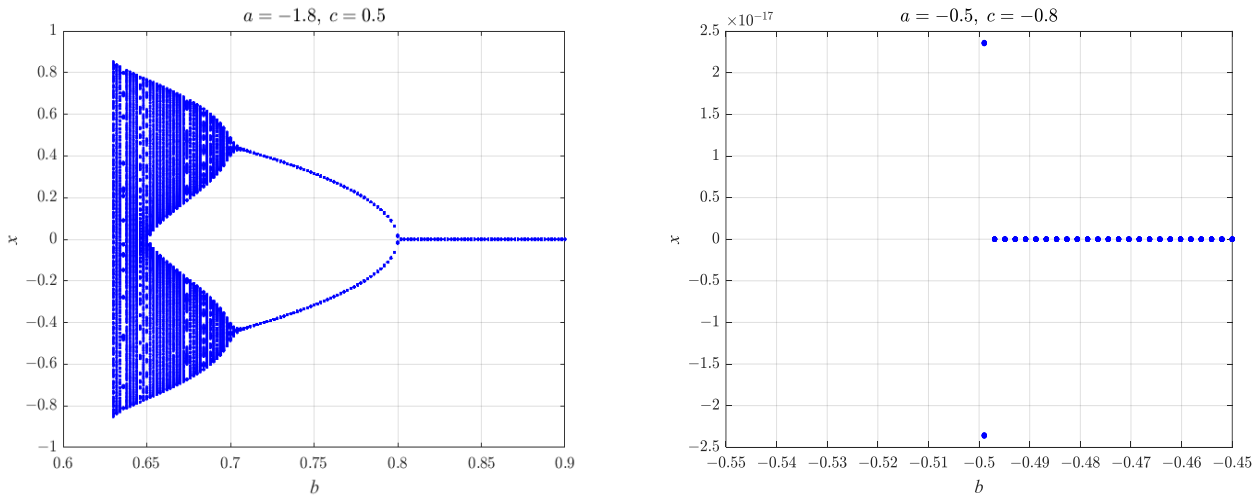

Figure 5. Output of the first component of the system state (x, y) with respect to b.

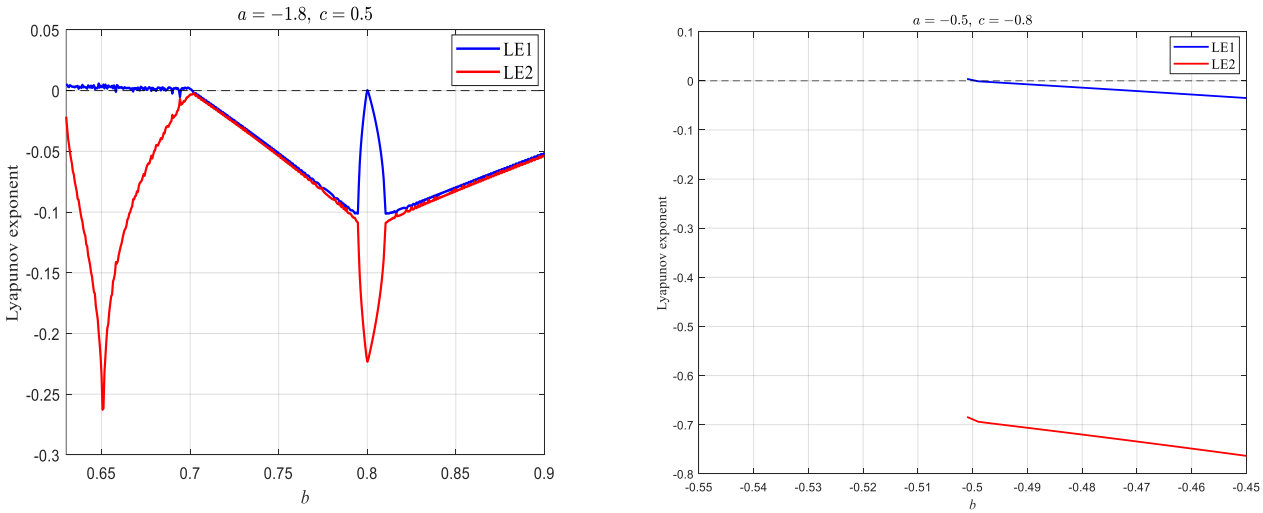

Figure 6. Lyapunov exponents of the discrete system (12) with respect to b.

3.2. Application analysis of bifurcations

In Section 3.1, the existence of bifurcations is analyzed theoretically and numerically. The theoretical analysis yields the critical value conditions under which discrete dynamical system (12) exhibits various bifurcations. Additionally, the correctness of the theoretical results is verified by several sets of numerical experiments. Some Lyapunov exponents of discrete system (12) are positive in Figures 2 and 6. They indicate that Neimark-Sacker bifurcation and period-doubling bifurcation are the way to induce the chaos. The chaotic sequence exhibits a high degree of randomness and unpredictability. These chaotic features provide the core support for the encryption algorithm and improve the anti-cracking ability of the encryption systems [29]. Hence, bifurcations of system (12) have significant application potential in image encryption.

To further validate the practical application potential of the bifurcation of system (12) in image encryption, the numerical experiments are presented in this section. When $a = –1.8$, $b = 0.8$, and $c = 0.4$, system (12) is used to generate pseudo-random sequences for pixel position permutation or pixel gray value encryption. The plaintext image is Peppers (512×512) in color. In image encryption, system (12) is iterated 500000 times. States of the first 1000 iterations are discarded, and the subsequent iterations' results are used in image encryption. Initial state is $x = 0.01$ and $y = 0.01$. Figure 7 shows the encryption effect. The number of pixel change rate (NPCR) in Figure 7 is 99.6126%, which is remarkably close to the theoretical optimum of approximately 99.6094% [30]. It is an ideal value, indicating that this encryption has extremely strong diffusion characteristics and sensitivity to plaintext. Figure 8 shows the encryption and decryption effect.

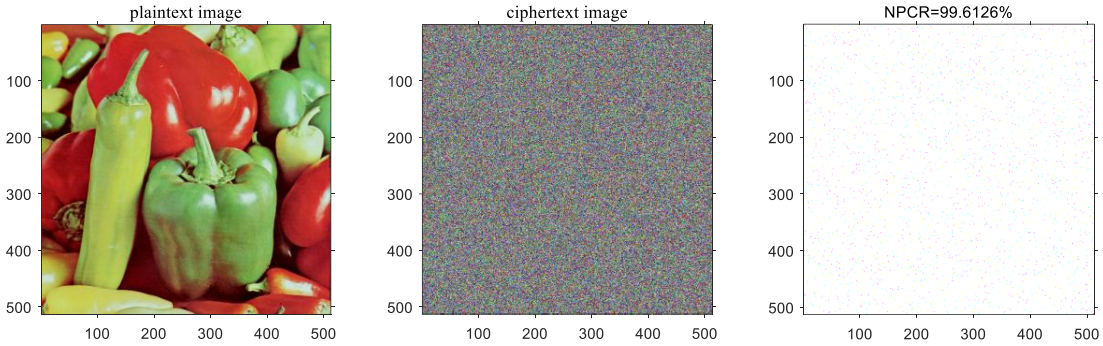

Figure 7. Encryption effect diagram with system (12).

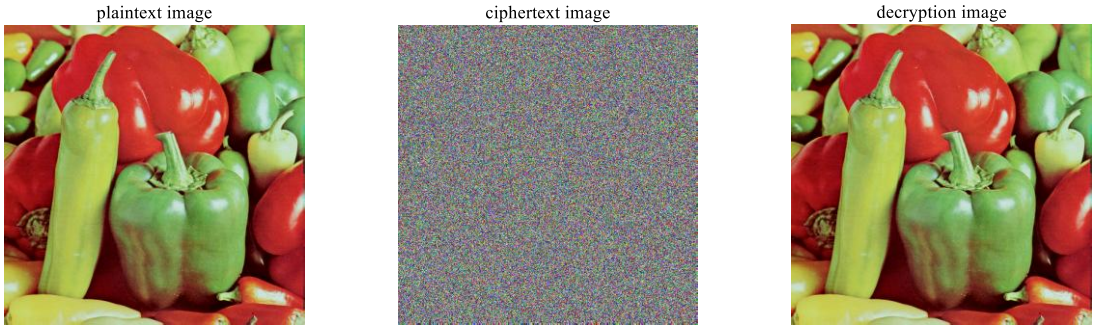

Figure 8. Encryption and decryption effect diagrams.

Tables 1 to 3 enumerate the correlation analysis results of this encryption. By comparing the plaintext images, the correlation of ciphertext images is approaching 0. This implies that the encryption utilizing system (12) enables invalid statistical attacks. Table 4 enumerates the results of the information entropy. Information entropy in the ciphertext image is approaching 8. This indicates a higher degree of information uncertainty in the ciphertext image. In this encryption experiment, the unified average changing intensity (UACI) is 32.2826%, which approaches the ideal theoretical benchmark of approximately 33.4%, confirming that the average intensity change is significant and uniform. These metrics confirm that the encryption utilizing system (12) effectively resists differential cryptanalysis. The security performance of image encryption utilizing system (12) demonstrates a high level of effectiveness.

Key sensitivity is a fundamental requirement for an ideal encryption scheme. Even if one bit of the key changes, the encryption results should be completely different. The key of this image encryption is composed of a random sequence generated by system (12). Moreover, the condition for the occurrence of period-doubling bifurcation in system (12) is $b = -a - 1$. Thus, the influential factors of the key include parameter a, c and the initial states of x, y. Based on these, key sensitivity is tested in two steps. First, each key component (parameters and initial states) is individually perturbed by a tiny value, with other components fixed. Then, the resulting divergence between the encrypted images is evaluated using NPCR and UACI. Table 5 enumerates the key sensitivity

analysis results of this encryption. Most parameters of this encryption exhibit good sensitivity, with a NPCR value close to 99.6% and UACI value around 33.4%. Since the first 1000 iteration results of system (12) are not used in key generation, the initial states of x, y exhibit low sensitivity under minor perturbations. The key generation algorithm is required to be optimized. Table 6 summarizes the performance comparison data of image encryption between system (12) and other systems. The comparative results indicate that the encryption effectiveness of system (12) is slightly superior to that of other systems.

Based on comprehensive analysis, bifurcations of system (12) are effective in image encryption.

Table 1. R-channel correlation.

	Horizontal correlation	Vertical correlation	Diagonal correlation
Plaintext image R-channel	0.9643	0.9644	0.9566
Ciphertext image R-channel	0.0007	0.0183	-0.0098

Table 2. G-channel correlation.

	Horizontal correlation	Vertical correlation	Diagonal correlation
Plaintext image G-channel	0.9814	0.9824	0.9685
Ciphertext image G-channel	0.0004	-0.0140	-0.0064

Table 3. B-channel correlation.

	Horizontal correlation	Vertical correlation	Diagonal correlation
Plaintext image B-channel	0.9637	0.9629	0.9423
Ciphertext image B-channel	0.0088	0.0194	-0.0158

Table 4. Information entropy.

Color Channel	Information Entropy
Plaintext image R-channel	0
Ciphertext image R-channel	7.9993
Plaintext image G-channel	0.3269
Ciphertext image G-channel	7.9993
Plaintext image B-channel	0.3075
Ciphertext image B-channel	7.9993

Table 5. Results of the sensitivity test.

Perturbation value	Test object	NPCR (%)	UACI (%)
10^{-11}	Initial value of x	34.1656	6.1697
	Initial value of y	67.3244	6.4206
	Parameter a	99.6426	33.3318
	Parameter c	99.6395	34.8203
10^{-8}	Initial value of x	99.6098	33.3773
	Initial value of y	99.6067	33.4090
	Parameter a	99.6010	33.4755
	Parameter c	99.5945	33.4924
10^{-5}	Initial value of x	99.5983	33.4936
	Initial value of y	99.6109	33.5144
	Parameter a	99.6010	33.3769
	Parameter c	99.5914	33.3390
10^{-2}	Initial value of x	99.6120	33.4309
	Initial value of y	99.6193	33.4427
	Parameter a	99.6067	33.4643
	Parameter c	99.6265	33.4665

Table 6. Performance comparison of image encryption.

System	NPCR (%)	UACI (%)	Information Entrpy (R-channel)	Information Entropy (G-channel)	Information Entropy (B-channel)
System (12)	99.6126	32.2826	7.9993	7.9993	7.9993
Ref. [8]	99.6042	32.2117	7.9994	7.9994	7.9993
Ref. [9]	99.6171	32.2603	7.9993	7.9993	7.9993
Ref. [31]	99.6076	32.2410	7.9992	7.9993	7.9992

4. Anti-control of bifurcations in two-dimensional, three-parameter discrete dynamical system with cubic terms

In Section 3, we demonstrate the practical value of the bifurcations of system (12) in image encryption. To broaden their applicability and enhance flexibility, the occurrence of bifurcation is required. Anti-control of bifurcations can achieve this purpose. Anti-control of bifurcations refers to the process of deliberately inducing desired bifurcations through control actions applied at pre-specified parameter values within a system. Rather than suppressing or avoiding bifurcations, this approach actively generates and harnesses bifurcation phenomena for beneficial applications in engineering and scientific domains. In this section, we focus on the design of the anti-control of bifurcations and verify the effectiveness of the proposed controller through numerical experiments.

4.1. Anti-control of Neimark-Sacker bifurcation

4.1.1. Design of the controller

Anti-control of the Neimark-Sacker bifurcation can actively and deliberately induce the occurrence of Neimark-Sacker bifurcation, thereby driving the system transition from simple dynamical behavior to complex dynamics. In this paper, a controller is designed using the state feedback method to perform anti-control on the Neimark-Sacker bifurcation of the two-dimensional three-parameter discrete dynamical system with cubic terms (12), which enables the Neimark-Sacker bifurcation to occur prematurely at a preset value.

For the discrete system (12), we aim to induce a Neimark-Sacker bifurcation at the fixed point $(0, 0)$ by applying anti-control, with the preset value as b_0. The controller of anti-control of the Neimark-Sacker bifurcation is designed as

$$\begin{cases} x \mapsto ax - y + u_1, \\ y \mapsto bx + cx^3 + u_2, \end{cases} \tag{28}$$

where $u_1 = k_1x + k_2y,\ u_2 = k_3x + k_4y.$

The control system (28) is described as

$$\begin{cases} x \mapsto ax - y + k_1x + k_2y, \\ y \mapsto bx + cx^3 + k_3x + k_4y. \end{cases} \tag{29}$$

Jacobian matrix of the control system (29) at the fixed point (0,0) is

$$J = \begin{pmatrix} a + k_1 & -1 + k_2 \\ b + k_3 & k_4 \end{pmatrix}. \tag{30}$$

The characteristic equation of the Jacobian matrix (30) is

$$\lambda^2 - (k_4 + a + k_1)\lambda + ak_4 + k_1k_4 + b + k_3 - bk_2 - k_2k_3 = 0\,. \tag{31}$$

In order to undergo the Neimark-Sacker bifurcation at $b = b_0$, controlled system (29) must satisfy the following conditions:

(1) The characteristic equation must have a pair of conjugate complex roots, that is

$$\Delta = (k_4 + a + k_1)^2 - 4(ak_4 + k_1k_4 + b_0 + k_3 - b_0k_2 - k_2k_3) < 0\,,$$

and

$$\lambda = \frac{k_4 + a + k_1 + \sqrt{(k_4 + a + k_1)^2 - 4(ak_4 + k_1k_4 + b_0 + k_3 - b_0k_2 - k_2k_3)}}{2},$$

$$\bar{\lambda} = \frac{k_4 + a + k_1 - \sqrt{(k_4 + a + k_1)^2 - 4(ak_4 + k_1k_4 + b_0 + k_3 - b_0k_2 - k_2k_3)}}{2}.$$

(2) $|\lambda(b_0)| = \sqrt{ak_4 + k_1k_4 + b_0 + k_3 - b_0k_2 - k_2k_3} = 1.$

(3) $\lambda^n(b_0) \neq 1,\ n = 1,2,3,4.$

(4) $\frac{d}{d(b)}|\lambda(b_0)| \neq 0.$

(5) $\alpha \neq 0.$

(6) The control system (29) is invertible, that is

$$k_2 = 1, a + k_1 \neq 0, k_4 \neq 0 \text{ or } k_2 \neq 1, [(a + k_1)k_4 - (k_2 - 1)(b_0 + k_3)] \cdot (k_2 - 1) \cdot c \leq 0.$$

Based on the aforementioned conditions, it can be concluded that the control parameters k_1, k_2, k_3, and k_4 must satisfy the following conditions:

$$\begin{cases} |k_1 + a| \neq \frac{1}{2}, \\ k_2 \neq 1, \\ |k_4| \neq \frac{1}{2}, \\ k_3 = \frac{1-(a+k_1)k_4}{1-k_2} - b_0, \\ -2 < a + k_1 + k_4 < 2, \\ ak_1 + ak_4 + k_1k_4 \neq 1, \\ (k_2 - 1) \cdot c < 0. \end{cases} \tag{32}$$

For the control system (29), when the control parameters k_1, k_2, k_3, $and\ k_4$ satisfy formula (32), the discrete system (29) will undergo a Neimark-Sacker bifurcation at the preset value b_0.

4.1.2. Numerical experiment

In this section, a series of numerical experiments are conducted to verify the effectiveness of the anti-controller of the Neimark-Sacker bifurcation. In Section 3.1, we discussed the Neimark-Sacker bifurcation of system (12) with $a = -0.2$ and $b = 0.4$, and clarified that when $b = 1$, system (12) undergoes a Neimark-Sacker bifurcation. To enable system (12) to trigger Neimark-Sacker bifurcation in advance at the preset value $b = 0.5$, we implement anti-control of Neimark-Sacker bifurcation on system (12). Control system (29) is

$$\begin{cases} x \mapsto -0.2x - y + k_1x + k_2y, \\ y \mapsto 0.5x + 0.4x^3 + k_3x + k_4y, \end{cases} \tag{33}$$

where $k_1 = -1$, $k_2 = 0.2$, $k_3 = 3.75$, $k_4 = 2$, and the initial state is $(0.001,0.001)$. Figure 9 is the phase diagram of control system (33). This indicates that when $b = 0.5$, control system (33) undergoes a Neimark-Sacker bifurcation at the fixed point (0,0).

To verify the robustness of the anti-controller of the Neimark-Sacker bifurcation, random

perturbations at varying levels (0%-10%) are applied to the control parameters k_1, k_2, k_3, and k_4 of system (33). For each perturbation level, 100 random trials are conducted. Figure 10 illustrates the trend of the mean bifurcation point deviation versus the perturbation level. Even under the maximum perturbation of 10%, the mean deviation remains at a low level. This indicates that the anti-controller (33) possesses good robustness against parameter uncertainties.

To thoroughly evaluate the influence of each control parameter k_1, k_2, k_3, and k_4, sensitivity analysis is conducted for each parameter individually. The sensitivity index (SI) is defined as

$$SI = \frac{\Delta b_0/b_0}{\triangle p/p}, \tag{34}$$

where b_0 is the preset bifurcation value ($b_0 = 0.5$), Δb_0 is the actual shift of the bifurcation point, and $\Delta p/p$ is the relative perturbation amplitude of the control parameter. For each parameter, 100 random perturbation trials are performed, and the average deviation is used to compute the sensitivity. When the perturbation level is 3%, the sensitivity indexes of k_1, k_2, k_3, and k_4 are 5.0000, 2.1333, 6.2667, and 5.5167, respectively. This result shows that parameter k_3 exhibits the highest sensitivity. This quantitative sensitivity analysis provides crucial guidance for practical implementation.

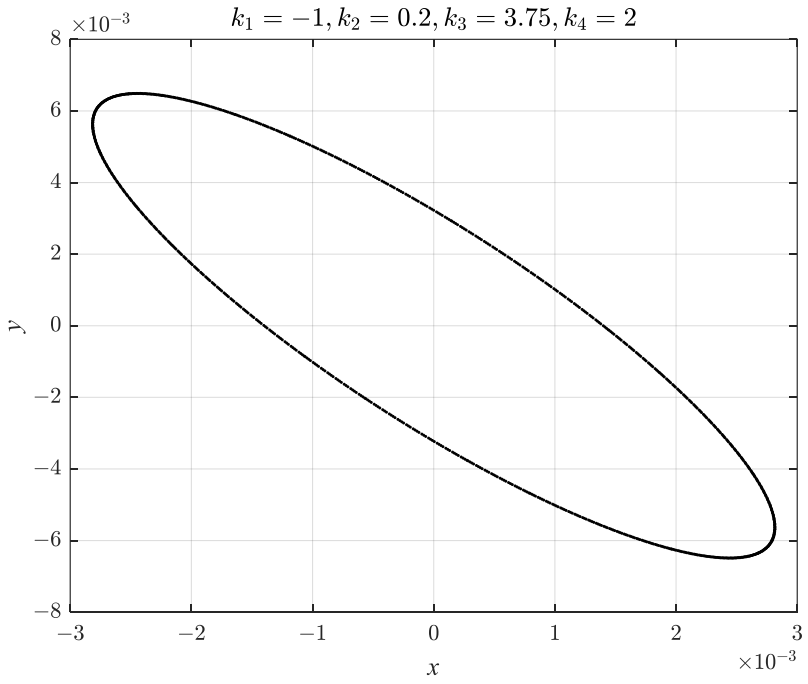

Figure 9. Phase diagram of control system (33).

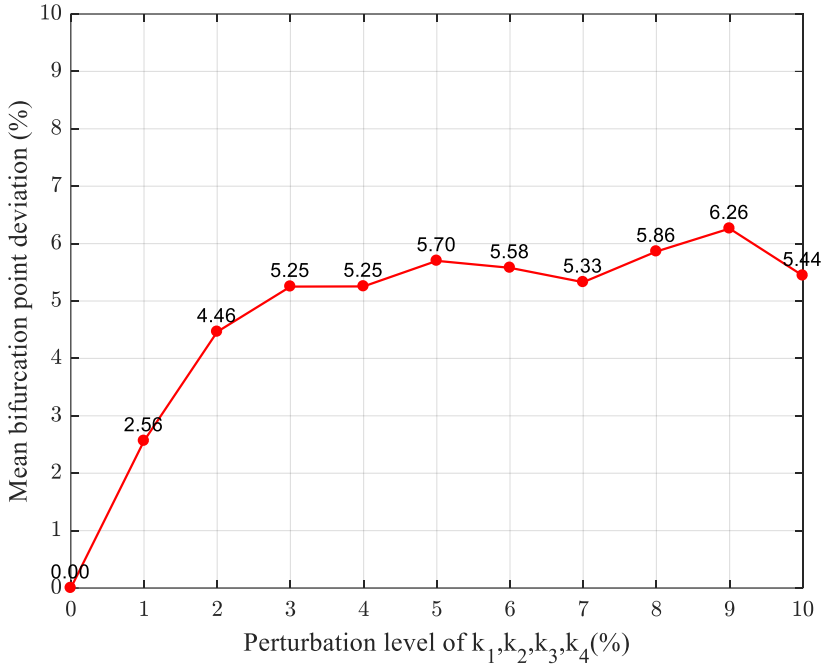

Figure 10. Robustness analysis diagram of control system (33).

4.2. Anti-control of period-doubling bifurcation

4.2.1. Design of the controller

In this section, we design the anti-controller of period-doubling bifurcation to induce a period-doubling bifurcation. Since we aim to induce a period-doubling bifurcation at the preset parameter value $b = b_0$, the anti-control system of period-doubling bifurcation is designed as

$$\begin{cases} x \mapsto ax - y + u_1, \\ y \mapsto bx + cx^3 + u_2, \end{cases} \tag{35}$$

where u_1 *and* u_2 are the controllers, $u_1 = k_1 x$, $u_2 = (b_0 - b + k_2)x$, and k_1, k_2 are the control parameters.

Based on Theorem 3.3, the parameters must satisfy the following conditions:

$$\begin{cases} b_0 + k_2 = -(a + k_1) - 1, \\ a + k_1 \neq -2, \\ (b_0 + k_2) \cdot c > 0. \end{cases} \tag{36}$$

4.2.2. Numerical experiment

To verify the effectiveness of anti-control of period-doubling bifurcation, a set of comparative experiments are conducted in this section. From Figure 5, when $a = -1.8, b = 0.8, c =$

$0.5, and\ u_1 = u_2 = 0$, discrete system (12) undergoes a period-doubling bifurcation at the fixed point (0,0). To enable system (12) to trigger a period-doubling bifurcation in advance at the preset value $b = 0.6$, anti-control of period-doubling bifurcation is applied. The control system is

$$\begin{cases} x \mapsto -1.8x - y + k_1 x, \\ y \mapsto x + 0.5x^3 + (k_2 - 0.4)x, \end{cases} \tag{37}$$

where $k_1 = 0.5$ and $k_2 = -0.3$. Figure 11 shows the variations of the first component of the system state (x, y) with respect to b. Thus, control system (37) undergoes a period-doubling bifurcation at $b = 0.6$.

To verify the robustness of the anti-controller of the period-doubling bifurcation, random perturbations at varying levels (0%-10%) are applied to the control parameters of system (37). For each perturbation level, 100 random trials are conducted. Figure 12 illustrates the trend of the mean bifurcation-point deviation versus the perturbation level. As the perturbation level increases from 0% to 10%, the mean bifurcation point deviation increases correspondingly from 0% to approximately 2.43%. Even under the maximum perturbation of 10%, the mean deviation remains at a low level. This indicates that the anti-controller (37) possesses good robustness against parameter uncertainties. To evaluate the influence of each control parameter k_1 and k_2, a sensitivity analysis is conducted for each parameter individually, which is computed with formula (34). The sensitivity index of k_1 is 1.6667. The sensitivity index of k_2 is 1. Parameter k_1 is more sensitive than k_2.

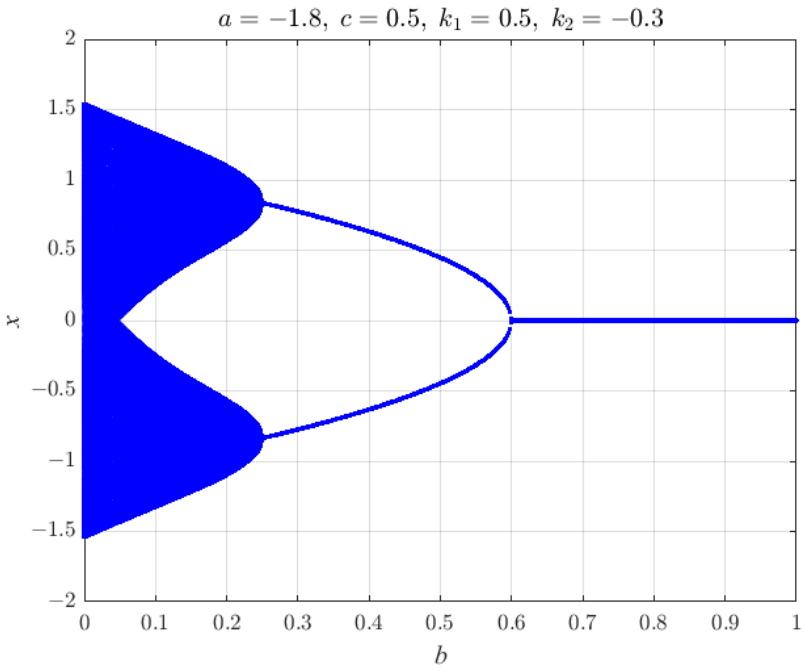

Figure 11. Output of the first component of (x, y) of system (37) with respect to b.

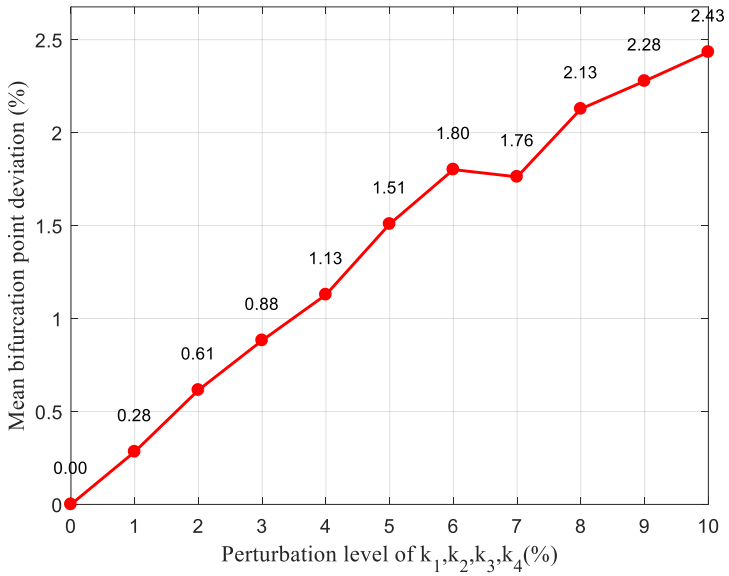

Figure 12. Robustness analysis diagram of control system (37).

5. Conclusions

In this paper, a class of two-dimensional, three-parameter discrete systems with cubic terms is presented. Existence and local stability conditions of the fixed points are analytically deduced in the proposed system, which establish a solid theoretical foundation for the bifurcations analysis. Furthermore, the bifurcations of proposed discrete system (12) are investigated through theoretical and numerical analyses. The critical parameter conditions for the onset of the Neimark-Sacker, pitchfork, and period-doubling bifurcations are derived through the theoretical derivation. Several numerical experiments are conducted in this paper. These simulations not only verify the correctness of the critical parameter conditions of bifurcations, but also show that proposed system (12) is suitable to be used in image encryption. Finally, one anti-controller is designed to induce Neimark-Sacker bifurcation at the predetermined parameter values, and the other anti-controller is designed to induce the period-doubling bifurcation. The anti-controllers combine the state feedback control method with the conditions of the bifurcations existence. Numerical simulations confirm the effectiveness and robustness of the proposed anti-controllers.

The two-dimensional, three-parameter discrete system with cubic terms has an asymmetric, invertible, and linear-nonlinear hybrid structure. This structure achieves linear cross-coupling by confining the cubic term to a single dimension. As a result, the system exhibits complex dynamical behaviors, laying a dynamical foundation for generating highly random and unpredictable sequences. To expand the key space and enhance real-time performance, we will focus on designing and optimizing more secure and computationally efficient key generation algorithms based on system (12) in the future.

Author contributions

Limei Liu, Jiangna Ruan, Jun Zhai, Xiuling Li: Conceptualization, methodology, software,

validation, writing—original draft preparation, writing—review and editing. All authors have read and approved the final version of the manuscript for publication

Use of Generative-AI tools declarations

The authors declare they have not used Artificial Intelligence (AI) tools in the creation of this article.

Conflict of interest

All authors declare no conflicts of interest in this paper.

References

1. W. L. Price, An algorithm which generates the Hamiltonian circuits of a cubic planar map, *J. London Math. Soc.*, **s2-18** (1978), 193–201. https://doi.org/10.1112/jlms/s2-18.2.193
2. R. M. May, Mathematical modelling: The cubic map in theory and practice, *Nature*, **311** (1984), 13–14. https://doi.org/10.1038/311013a0
3. R. M. May, Nonlinear phenomena in ecology and epidemiology, *Ann. N. Y. Acad. Sci.*, **357** (1980), 267–281. https://doi.org/10.1111/j.1749-6632.1980.tb29692.x
4. T. D. Rogers, D. C. Whitley, Chaos in the cubic mapping, *Math. Model.*, **4** (1983), 9–25. https://doi.org/10.1016/0270-0255(83)90030-1
5. O. Chavoya-Aceves, F. Angulo-Brown, E. Pina, Symbolic dynamics of the cubic map, *Phys. D*, **14** (1985), 374–386. https://doi.org/10.1016/0167-2789(85)90096-X
6. A. Munteanu, E. Petrisor, E. García-Berro, J. José, Creation of twistless circles in a model of stellar pulsations, *Commun. Nonlinear Sci. Numer. Simul.*, **8** (2003), 355–373. https://doi.org/10.1016/S1007-5704(03)00054-6
7. Y. G. Shi, L. Chen, Reversible maps and their symmetry lines, *Commun. Nonlinear Sci. Numer. Simul.*, **16** (2011), 363–371. https://doi.org/10.1016/j.cnsns.2010.04.012
8. Y. Gao, Complex dynamics in a two-dimensional noninvertible map, *Chaos Solitons Fract.*, **39** (2009), 1798–1810. https://doi.org/10.1016/j.chaos.2007.06.051
9. D. Ilhem, K. Amel, One-dimensional and two-dimensional dynamics of cubic maps, *Discrete Dyn. Nat. Soc.*, **2006** (2006), 015840. https://doi.org/10.1155/DDNS/2006/15840
10. Y. Zhang, G. Luo, Wada bifurcations and partially Wada basin boundaries in a two-dimensional cubic map, *Phys. Lett. A*, **377** (2013), 1274–1281. https://doi.org/10.1016/j.physleta.2013.03.027
11. M. Gonchenko, S. Gonchenko, I. Ovsyannikov, Bifurcations of cubic homoclinic tangencies in two-dimensional symplectic maps, *Math. Model. Nat. Phenom.*, **12** (2017), 41–61. https://doi.org/10.1051/mmnp/201712104
12. M. Gonchenko, S. V. Gonchenko, I. Ovsyannikov, A. Vieiro, On local and global aspects of the 1:4 resonance in the conservative cubic Hénon maps, *Chaos*, **28** (2018), 043123. https://doi.org/10.1063/1.5022764
13. M. S. Gonchenko, A. O. Kazakov, E. A. Samylina, A. Shykhmamedov, On 1:3 resonance under reversible perturbations of conservative cubic Hénon maps, *Regul. Chaotic Dyn.*, **27** (2022), 198–216. https://doi.org/10.1134/S1560354722020058

14. Y. N. Xing, J. Zeng, W. Dong, J. Zhang, P. Guo, Q. Ding, Hybrid synchronisation method based on inverse generalised and inverse projected high dimensional discrete chaotic systems, *Phys. Scr.*, **99** (2024), 035231.
15. G. C. Wu, H. S. Hou, R. Lozi, Neimark-Sacker bifurcation of discrete fractional chaotic systems, *Internat. J. Bifur. Chaos*, **35** (2025), 2550049. https://doi.org/10.1142/S021812742550049X
16. K. Mokni, A. A. Thirthar, M. Ch-Chaoui, S. Jawad, M. A. Abbasi, Stability and bifurcation analysis in a novel discrete prey-predator system incorporating moonlight, water availability, and vigilance effects, *Int. J. Dynam. Control*, **13** (2025), 219. https://doi.org/10.1007/s40435-025-01718-2
17. K. Mokni, M. Ch-Chaoui, B. Mondal, U. Ghosh, Rich dynamics of a discrete two dimensional predator–prey model using the NSFD scheme, *Math. Comput. Simulation*, **225** (2024), 992–1018. https://doi.org/10.1016/j.matcom.2023.09.024
18. B. Xin, T. Chen, J. Ma, Neimark-Sacker bifurcation in a discrete-time financial system, *Discrete Dyn. Nat. Soc.*, **2010** (2010), 405639. https://doi.org/10.1155/2010/405639
19. G. Vivekanandhan, H. R. Abdolmohammadi, H. Natiq, K. Rajagopal, S. Jafari, H. Namazi, Dynamic analysis of the discrete fractional-order Rulkov neuron map, *Math. Biosci. Eng.*, **20** (2023), 4760–4781. https://doi.org/10.3934/mbe.2023220
20. P. C. Bressloff, S. Coombes, A dynamical theory of spike train transitions in networks of integrate-and-fire oscillators, *SIAM J. Appl. Math.*, **60** (2000), 820–841. https://doi.org/10.1137/S0036139998339643
21. A. Aloui, L. Diabi, O. Kahouli, A. Ouannas, L. El Amraoui, M. Ayari, Chaotic dynamics, complexity analysis and control schemes in fractional discrete market system, *Fractal Fract.*, **9** (2025), 721. https://doi.org/10.3390/fractalfract9110721
22. L. Liu, X. Zhong, Research on stability and bifurcation for two-dimensional two-parameter squared discrete dynamical systems, *Mathematics*, **12** (2024), 2423. https://doi.org/10.3390/math12152423
23. M. B. Almatrafi, M. Berkal, R. Ahmed, Dynamical transitions and chaos control in a discrete predator-prey model with Gompertz growth and Holling type III response, *Chaos Solitons Fract.*, **200** (2025), 117071. https://doi.org/10.1016/j.chaos.2025.117071
24. Y. Chen, Z. Yu, Y. Li, J. Yu, Controlling bifurcations in duffing mapping, *Bull. Malays. Math. Sci. Soc.*, **48** (2025), 209. https://doi.org/10.1007/s40840-025-01993-4
25. L. Liu, X. Zhong, Analysis and anti-control of period-doubling bifurcation for the one-dimensional discrete system with three parameters and a square term, *AIMS Mathematics*, **10** (2025), 3227–3250. https://doi.org/10.3934/math.2025150
26. X. Wu, G. Wen, H. Xu, L. He, Anti-controlling Neimark-Sacker bifurcation of a three-degree-of-freedom vibration system with clearance, (in chinese), *Acta Phys. Sin.*, **64** (2015), 200504. https://doi.org/10.7498/aps.64.200504
27. J. Guckenheimer, P. Holmes, Nonlinear oscillations, dynamical systems, and bifurcations of vector fields, In: *Applied mathematical sciences*, New York: Springer, 1983. https://doi.org/10.1007/978-1-4612-1140-2
28. S. Wiggins, Introduction to applied nonlinear dynamical systems and chaos, In: *Texts in applied mathematics*, New York: Springer, 1990. https://doi.org/10.1007/978-1-4757-4067-7

29. M. Zhao, L. Li, Z. Yuan, An image encryption approach based on a novel two-dimensional chaotic system, *Nonlinear Dyn.*, **112** (2024), 20483–20509. https://doi.org/10.1007/s11071-024-10053-8
30. H. Liu, J. Liu, C. Ma, Constructing dynamic strong S-Box using 3D chaotic map and application to image encryption, *Multimed. Tools Appl.*, **82** (2023), 23899–23914. https://doi.org/10.1007/s11042-022-12069-x
31. X. Wang, X. Xu, K. Sun, Z. Jiang, M. Li, J. Wen, A color image encryption and hiding algorithm based on hyperchaotic system and discrete cosine transform, *Nonlinear Dyn.*, **111** (2023), 14513–14536. https://doi.org/10.1007/s11071-023-08538-z

AIMS Press